# The influence of post-heat treatments on the tensile strength and surface hardness of selectively laser-melted AlSi10Mg

## Author

Heilgeist, S, Heine, B, Merkel, M, Hitzler, L, Javanbakht, Z, Öchsner, A

## Published

2019

## Journal Title

Materialwissenschaft und Werkstofftechnik

## Version

Accepted Manuscript (AM)

## DOI

https://doi.org/10.1002/mawe.201800236

## Copyright Statement



## Downloaded from



## Griffith Research Online

# *This is the post-print version of the following article:*

Hitzler, L., Charles, A., Öchsner, A., 2016. The Influence of Post-Heat-Treatments on the Tensile Strength and Surface Hardness of Selective Laser Melted AlSi10Mg. Defect and Diffusion Forum 370, 171-176.

http://dx.doi.org/10.4028/www.scientific.net/DDF.370.171.

# The influence of post-heat-treatments on the tensile strength and surface hardness of selective laser melted AlSi10Mg

Leonhard Hitzler[1,a *], Amandine Charles[2,b] and Andreas Öchsner[1,c]

[1]Griffith University, Griffith School of Engineering, Southport 4222, Australia
[2]Université de Toulon, SeaTech School of Engineering, 83957 La Garde Cedex, France

[a]Leonhard.Hitzler@Griffithuni.edu.au, [b]Amandine.Charles.17@seatech.fr,
[c]A.Oechsner@Griffith.edu.au

**Keywords:** Additive Manufacturing, Powder-bed, Anisotropy, Alignment, Precipitation Hardening, Dwell Time, Homogenization

**Abstract.** Recent investigations revealed major fluctuations in the material properties of selective laser melted AlSi10Mg, which corresponded with the varying precipitation-hardening state of the microstructure, caused by the differing dwell times at elevated temperatures. It was indicated that a subsequent heat treatment balances the age-hardening and results in a homogenized material strength. In order to further investigate this statement selective laser melted AlSi10Mg samples were subject to multiple post-heat-treatments. Subsequently, the surface hardness and tensile strength was determined and compared with the as-built results. The post-heat-treatment led to an arbitrary occurrence of rupture, indicating a successful homogenization, coupled with a remarkable improvement in ductility, but to the costs of a lowered tensile strength, which was highly dependent on the chosen heat-treatment procedure.

## Introduction

The selective laser melting (SLM) process belongs to the family of layer-wise, powder-bed based additive manufacturing technologies and evolved from the older selective laser sintering (SLS) process [1]. Commonly, the information for production, required for the description of the irradiation, is gained by the conversion of the CAD-data into a sliced model with equally thick sections. The thickness of these slices describes the powder layer thickness required in the manufacturing process. Based on the cross-sections of the individual slices and the selected irradiation strategy the irradiation paths and sequences are obtained. During the manufacturing process the part is generated as a sequence of individual layers by successively adding powder layers and locally solidifying them with a laser beam [2]. This layer-wise approach enables high flexibility in geometry and design on one hand, but causes multiple directional dependencies on the other. Amongst the most important ones are the anisotropic mechanical properties [3,4] and the orientation and location dependent surface roughness [5,6].

The main distinction between SLS, SLM and other related processes is given by the binding mechanism of the powder particles [7]. The full melting of the raw material in SLM enables this process of manufacturing almost full dense parts without the need of a subsequent infiltration step.

However, in order to achieve these results, plenty of adjustments and optimizations were undertaken [8,9] and control mechanisms like the substrate plate heating were introduced [10].

Given the corresponding elevated temperatures present in the build environment, coupled with the long production times, alloys prone to microstructure alterations driven by heat input tend to locally change their properties. For the considered precipitation-hardenable AlSi10Mg alloy these inhomogeneities caused by varying age-hardening states were documented in [3]. The surface hardness and tensile strength was found to alter in the manufacturing environment. Based on the generation process with subsequent layers, this occurring alteration of properties with time is equivalent to a height dependent variation in material strength. This previous study also suggests that these inhomogeneities can be reduced or even equalized with subsequent post-heat-treatments, which represents the main focus of this study.

## Methods

### Manufacturing conditions.

The samples were produced with a SLM 280HL machine (SLM Solutions AG, Lübeck, Germany), which comprises a 400 W Yb-fibre-laser and offers a maximum build space of 280 x 280 x 320 mm³. Nitrogen was utilized as inert gas and the temperature regulation on the mounting plate[1] was set to 200°C. The block type support structure (i.e. a honeycomb scaffold) was chosen for the connection of the samples with the substrate plate (Figure 1).

(a) (b)

Figure 1: Support structure type "block"; (a) as received after SLM job, (b) sample removed

### Geometry, positioning and inclination.

The flat tensile samples type E 5 x 10 x 40, according to the German standard DIN 50125:2009-07, were chosen and produced with an oversize of 0.4 mm for subsequent machining and removal of surface influences.

On a side note, components fabricated with SLM are likely to inhabit an increased porosity right underneath the surface [11,12]; thus, for extensive loading and destructive material tests it is recommended to remove these crack initiation factors [13,14]. However, a subsequent machining step reduces the flexibility of the design, as it requires the accessibility with tools. For applications where the geometrical freedom is of higher importance as the removal of the porosity, e.g. in applications where the occurring stresses are uncritical, the surface quality can be enhanced with laser polishing [15,16].

In order to gain insight into the variance related to the build direction, the samples were produced in three representative configurations (Table 1), defined by the angle of the specimen's longitudinal axis to the substrate plate (xy-plane).

[1] The mounting plate is underneath the removable substrate plate and includes the thermal regulation.

Table 1: Positioning of the configurations in relation to the substrate plate

| Configuration | $\alpha_{XY}$ |
|---|---|
| **(a)** | 0° |
| **(b)** | 45° |
| **(c)** | 90° |

**Post heat treatment.**
In order to examine the effects of thermal treatment procedures three distinct heat-treatments were selected (Table 2), which varied mainly in the solution annealing temperature and duration.

Table 2: Considered heat-treatments

| Heat treatment | Solution annealing | Quenching | Thermal aging |
|---|---|---|---|
| **HT 1** | 6h - 525°C | water 25°C | 6h - 165°C |
| **HT 2** | 6h - 300°C | water 25°C | 6h - 180°C |
| **HT 3** | 4h - 500°C | water 25°C | 6h - 180°C |

## Material testing

**Surface hardness.**
The surface hardness was evaluated on the clamping areas of the tensile samples. It was ensured that the multiple indentations on each location (total of four investigated areas per sample) were performed in a reasonable distance to the edges and neighbouring indentations. The employed hardness testing machine (Wilson VH1150, ITW Buehler Group, MA, USA) was operated manually.

Figure 2: Hardness tester

**Tensile testing.**
The destructive material tests were performed on a tensile test machine (Instron, MA, USA) with a maximum load of 30 kN (Figure 3). The tensile tests were carried out in accordance to the German standard DIN EN ISO 6892-1:2009-12 with the crosshead speed set to 5 mm/min. In addition to the pure crosshead movement, the elongation of the specimen was measured with an extensometer with an initial distance of 25 mm.

Figure 3: Tensile test setup

## Results and discussion

### Surface hardness.

The surface hardness for the non-heat-treated samples was shown being dependent on the particular surface orientation and the positioning of the sample in the build space [3]. For the heat-treated samples this effect vanishes due to the equalizing of the precipitation-hardening state and thus, the global surface hardness, which represents the averaged hardness value based on multiple measurements on four clamping areas per considered sample, was seen as sufficiently accurate to characterize the hardness results (Table 3). HT 1 and HT 2 were found to lead to a drastic decrease in the hardness, whereas HT 3 only showed very minor changes compared to the hardness of the untreated reference samples.

Table 3: Global hardness in relation to the heat-treatment and configuration

| Configuration | Vickers Hardness in [HV3] | | | |
|---|---|---|---|---|
| | no HT | HT 1 | HT 2 | HT 3 |
| (a) | 115 | 56 | 66 | 110 |
| (b) | 118 | 52 | 70 | 110 |
| (c) | 107 | 51 | 63 | 109 |

### Tensile testing.

The tensile tests confirmed the tendencies revealed in the hardness investigation in terms of the ultimate tensile strength (UTS or $R_m$). Out of this it clearly can be concluded that the hardness and UTS are directly linked and can be targeted and adjusted dependent on the specific needs by choosing an adequate post-heat-treatment (Figure 4). Interestingly, the yield strength ($R_{p0.2}$) exhibited for the HT 3 samples exceeded the initial yield strength of the untreated samples on all configurations. All heat-treatments led to an improvement regarding the breaking elongation, with the best and most consistent results recorded for HT 2. This gain in ductility was clearly evident, the reference samples (no HT) ruptured without prior necking, whereas the heat-treated samples experienced localized necking. In addition, the tendency to fail towards the top end, documented in [3], was evident for the reference samples of configuration (b) and (c). The heat-treated samples on the other hand exhibited an arbitrary occurrence of rupture, thus proving the anticipated homogenizing effect of the heat-treatment procedures on the microstructure of the precipitation-hardenable AlSi10Mg alloy.

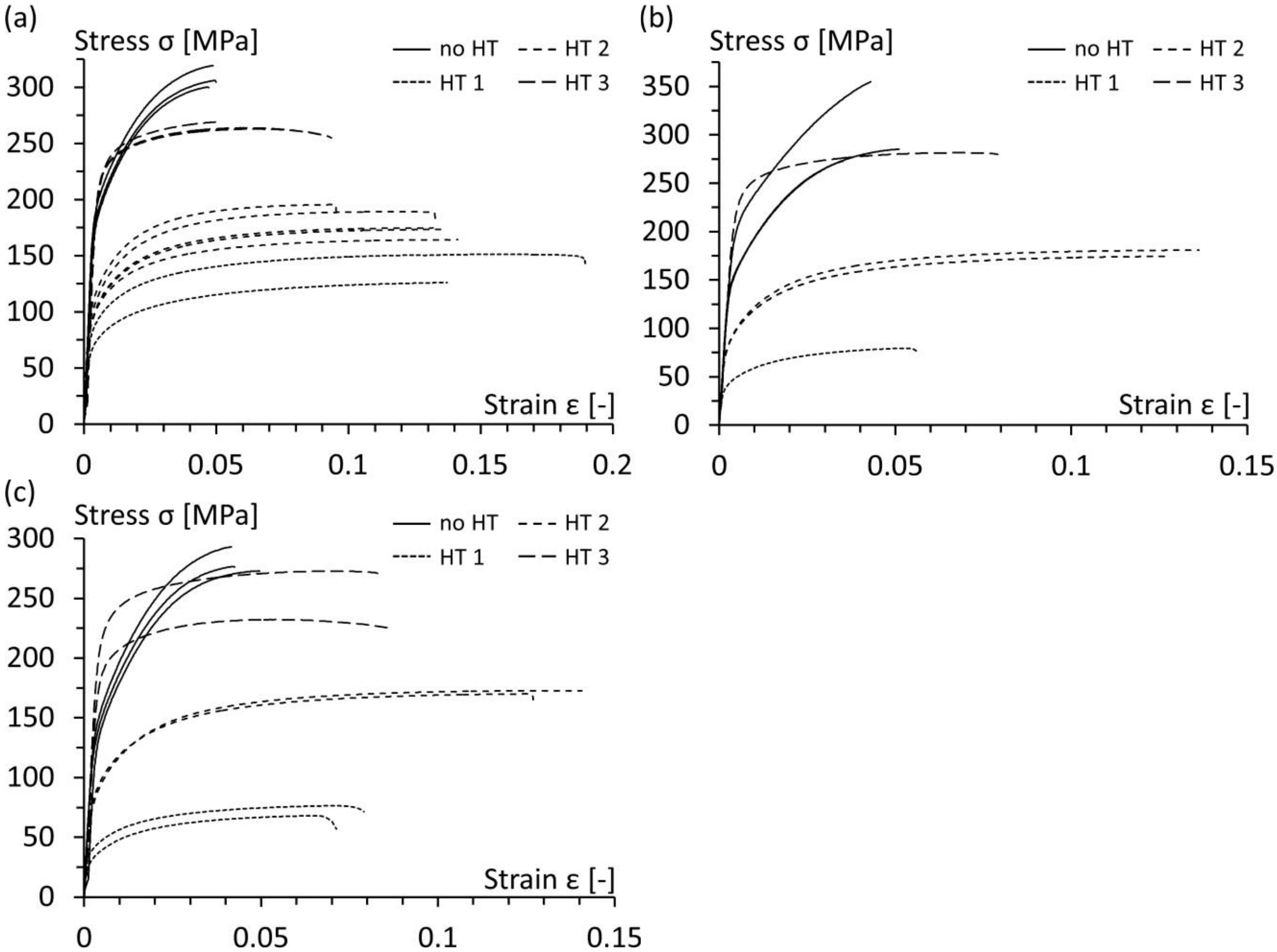

Figure 4: Stress-strain diagrams of the destructive tensile tests for all considered heat-treatment conditions grouped corresponding to configurations (a) to (c)

**Conclusion**

The selective laser melting procedure results in an anisotropic material behaviour with heterogeneous properties of fabricated components. It was shown that for the precipitation-hardenable AlSi10Mg these heterogeneities, reasoned in the dissimilar age-hardening states, could be homogenized with appropriate post-heat-treatments. Furthermore, the results presented indicate that the mechanical properties of selective laser melted AlSi10Mg can be adjusted in a targeted way by utilizing post-heat-treatments.

**Acknowledgement**

Sincere appreciation to Prof. Markus Merkel and his team at the University of Applied Sciences Aalen, Germany, for the supply of test specimens and their helpful support.

**References**

[1] I. Gibson, D.W. Rosen, B. Stucker, Additive Manufacturing Technologies. Springer-Verlag US, 2010.

[2] G.N. Levy, The role and future of the Laser Technology in the Additive Manufacturing environment. Physics Procedia 5, Part A (2010) 65-80.

[3] L. Hitzler, C. Janousch, J. Schanz, M. Merkel, B. Heine, F. Mack, W. Hall, A. Öchsner, Direction and location dependency of selective laser melted AlSi10Mg specimens. J Mater Process Technol 242 (2017) 48-61.

[4] L. Hitzler, J. Hirsch, J. Schanz, B. Heine, M. Merkel, W. Hall, A. Öchsner, Fracture toughness of selective laser melted AlSi10Mg. P I Mech Eng L: J Mat IN PRESS (2017).

[5] L. Hitzler, C. Janousch, J. Schanz, M. Merkel, F. Mack, A. Öchsner, Non-destructive evaluation of AlSi10Mg prismatic samples generated by Selective Laser Melting: Influence of manufacturing conditions. Mat-wiss u Werkstofftech 47 (2016) 564-581.
[6] L. Hitzler, J. Hirsch, M. Merkel, W. Hall, A. Öchsner, Position dependent surface quality in Selective Laser Melting. Mat-wiss u Werkstofftech 48 (2017) 327-334.
[7] J.P. Kruth, G. Levy, F. Klocke, T.H.C. Childs, Consolidation phenomena in laser and powder-bed based layered manufacturing. CIRP Ann Manuf Techn 56 (2007) 730-759.
[8] K. Kempen, L. Thijs, E. Yasa, M. Badrossamay, W. Verheecke, J.P. Kruth, Process optimization and microstructural analysis for selective laser melting of AlSi10Mg.
[9] D. Buchbinder, W. Meiners, E. Brandl, F. Palm, K. Müller-Lohmeier, M. Wolter, C. Over, W. Moll, J. Weber, N. Skrynecki, J. Grad, V. Neubert (2010) Abschlussbericht - Generative Fertigung von Aluminiumbauteilen für die Serienproduktion, 01RIO639A-D, BMBF. Projekt - AluGenerativ. Fraunhofer ILT, Aachen, Germany
[10] D. Buchbinder, W. Meiners, K. Wissenbach, R. Poprawe, Selective laser melting of aluminum die-cast alloy—Correlations between process parameters, solidification conditions, and resulting mechanical properties. J Laser Appl 27 (2015) S29205.
[11] N.T. Aboulkhair, N.M. Everitt, I. Ashcroft, C. Tuck, Reducing porosity in AlSi10Mg parts processed by selective laser melting. Addit Manuf 1-4 (2014) 77-86.
[12] K. Kempen, L. Thijs, J. Van Humbeeck, J.P. Kruth, Mechanical Properties of AlSi10Mg Produced by Selective Laser Melting. Physics Procedia 39 (2012) 439-446.
[13] B. Heine, Werkstoffprüfung - Ermittlung von Werkstoffeigenschaften, 2 edn. Carl Hanser Verlag, 2011.
[14] A. Öchsner, Continuum Damage and Fracture Mechanics. Springer, Singapur, 2016.
[15] J. Schanz, M. Hofele, L. Hitzler, M. Merkel, H. Riegel Laser polishing of additive manufactured AlSi10Mg parts with an oscillating laser beam. In: Machining, Joining and Modifications of Advanced Materials. Springer, Singapore, 2016, pp 159-169.
[16] J. Schanz, M. Hofele, S. Ruck, T. Schubert, L. Hitzler, G. Schneider, M. Merkel, H. Riegel, Metallurgical Investigations of Laser Remelted Additively Manufactured AlSi10Mg Parts. Mat-wiss u Werkstofftech 48 (2017) 463-476.